Journal of Illusion

PHENOMENAL REPORTS

Illusory lightness and contour formation through contrast modulation in novel Starburst illusions

David Flaieh*

Independent Researcher

Abstract

This article reviews historical lightness- and contour-based illusions and introduces several novel ones, including the Aquarius Starburst (Variants A and B), the Contrast-Enhanced Ellipse, the Pisces Starburst (Variants A and B), the Orion Starburst (Variants A and B), and additional related configurations. Systematic manipulations of contrast, luminance polarity, and geometry reveal recurring mechanisms, including lightness–contour–contrast interaction, lightness assimilation and contrast, transparency, the luminance-contrast convergence effect, polarity-preserving contour completion, and contrast-driven lightness–contour coactivation. This work further demonstrates uni- and bidirectional ray-beam effects and shows how bidirectional ray-beams become unidirectional and vice versa through polarity blocking, compression, rotation, or motion. Together, these findings provide a methodological tool for analyzing how contrast and polarity organize emergent contours and lightness percepts.

Keywords: *Visual illusion; illusory contours; lightness perception; lightness assimilation; lightness contrast; contour completion; Starburst illusion; ray-beam effect*.

Received: 17 December 2025; Revised: 1 August 2026; Accepted: 18 August 2026; Published: 25 November 2026

Edited by:
Akiyoshi Kitaoka

Reviewed by:
Sergio Roncato;
Gianni A. Sarcone

The Hermann Grid Illusion, first described by Ludimar Hermann in 1870, features white lines on a black background, where illusory gray spots appear at intersections and vanish with direct fixation (Hermann, 1870). Ewald Hering later documented the reversed polarity, leading to the term Hermann–Hering Illusion (Hering, 1872). Earlier observations were reported by David Brewster (1844), based on Reverend W. Selwyn's discovery, but Hermann (1870) established the classical form and its modern name. In 1941, Walter H. Ehrenstein introduced a similar lightness illusion in Modifikationen der Helligkeitserscheinung von L. Hermann, later termed the Ehrenstein illusion (Ehrenstein, 1941). Lines surrounding an empty center produce shifts in perceived lightness and illusory contours. Like the Kanizsa Triangle described by Gaetano Kanizsa in 1976, it shows how the brain constructs shape and lightness from incomplete visual input (Gregory, 1997; Kanizsa, 1976). In 2004, Victor de Lafuente and Octavio Ruiz showed that rotating the Hermann Grid Illusion by 45° reduces its strength to roughly one third of its classical form (de Lafuente & Ruiz, 2004), underscoring the illusion's orientation dependence. In 1993, Italian artist and researcher Gianni A. Sarcone began to popularize a polar variant of the Hermann–Hering Illusion (Fig. 1). Rotating the square 45° into a diamond and mapping it into polar coordinates reduced the usual intersection scintillations and introduced a new phenomenon: radial luminous streaks emanating from the figure. Sarcone named this effect ray-beams, also known as the Scintillating Starburst Illusion (Sarcone, 1993, 2021; Vicario, 2009).

The illusion created by Gianni A. Sarcone aligns with earlier findings traceable to Prandtl's (1927) work, who

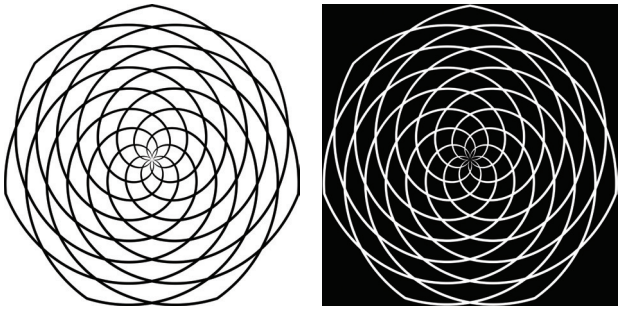

Fig. 1. Scintillating ray-beams and Starburst illusion by Gianni A. Sarcone. This illusion is featured in his book EyeTricks (2001–2007). The black grid produces light contours, and the white grid produces dark ones.

*Correspondence: David Flaieh. Email: davidflaieh@hotmail.com

Journal of Illusion 2026. © 2026 David Flaieh. This is an Open Access article distributed under the terms of the Creative Commons CC-BY-NC-ND 4.0 license (https://creativecommons.org/licenses/by-nc-nd/4.0/), allowing third parties to copy and redistribute the material in any medium or format and to remix, transform, and build upon the material for any purpose, even commercially, provided the original work is properly cited and states its license.

observed illusory vertical and horizontal light lines connecting the intersections of a 45-degree diagonal black grid, which he termed 'Spinnwebfäden', meaning spider's web threads or cobwebs (Prandtl, 1927). In 1950, Koiti Motokawa described an opposite-polarity variant in which illusory black lines appear to connect the intersections of white stripes in a modified Hermann grid, where the square elements are transformed into rhombuses (Motokawa, 1950). In 1976, R. A. Schachar introduced the pincushion-grid illusion, referring to Prandtl's lines as the 'pincushion grid' illusion and examining the phenomenon computationally (Schachar, 1976). Among comparable illusions is Jacques Ninio's (2001) 'flashing-lines' illusion, in which a periodic pattern of quadrangles produces pulsating illusory lines (Ninio, 2001). In the 2000s, Gianni A. Sarcone introduced a colored variant of the Scintillating Starburst, later documented as the Ghost-Color Variant (Sarcone, 2021). Earlier, Redies and Spillmann (1981) showed that Van Tuijl's neon-color effect (van Tuijl, 1975) emerges in the Ehrenstein figure when a colored cross connects the arms of the black lines across the central opening (Redies & Spillmann, 1981). The illusion parallels Kitaoka's Colored-Ray Illusion (Kitaoka, 2001), categorized as the 'pincushion-grid illusion of neon-color spreading', and falls within visual-completion phenomena alongside neon-color spreading (van Tuijl, 1975; Varin, 1971), the Ehrenstein figure (Ehrenstein, 1941), and the Kanizsa triangle (Kanizsa, 1976).

Aquarius Starburst illusion – Variant A

This article shows that the combined proceedings of illusory contours and lightness effects, summarized as the ray-beam effect produced by the 45° rotated grid, can be amplified through manipulation of geometry, contrast, and polarity ordering, giving rise to the Aquarius Starburst Illusion – Variants A and B. Named after Aquarius, one of the 88 constellations defined by the International Astronomical Union (Delporte, 1930), the illusion reflects perceptual qualities of flow and movement traditionally associated with the constellation.

The illusion's basic element is constructed by drawing an unfilled, black-lined outer square rotated 45°, together with a smaller, filled white inner square – also rotated 45° and positioned centrally to enhance contrast efficiency (Fig. 2, left). When the arrangement is inverted, it produces a pattern of opposite polarity (Fig. 2, right). The basic element, which can induce an illusory effect on its own, can also be arranged to construct a grid. The results show enhancements in perceived lightness and illusory contours that are horizontally and vertically connected to the grid, with white markers strengthening the black grid's light illusory contours, while black markers strengthen the white grid's dark illusory contours. The Spinnwebfäden illusion (Prandtl, 1927) consists solely of an empty black

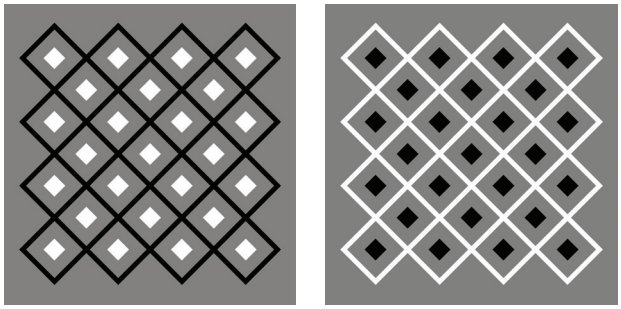

Fig. 2. Aquarius Starburst – Variant A: light illusory lines appear on the left and dark ones on the right, extending from the diamond's bisector.

grid that generates light contours and appears strongly only on a white background, whereas a gray background yields a weak effect. In comparison, the Aquarius Starburst – Variant A is presented on a gray background, which – without the white markers – produces a reduced illusory effect (Fig. 2, left). The perceptual effect is strongest when the four corners of the innermost 45° rotated squares are precisely aligned with the four corners of the outermost 45° rotated squares and weakens when they are displaced from this alignment. Further investigation focuses on adjustable variables that modulate and strengthen the illusory effect: (1) Outermost 45° rotated squares: varying line thickness can strengthen the ray-beam effect – for example, by drawing an adjacent square with different line weights. (2) Innermost 45° rotated squares: adjusting their size not only determines the intensity when modulating via spatial distance but also enhances contrast efficiency. (3) Distribution of the innermost 45° rotated squares: one square is left empty, while the other contains an inner marker, not only strengthening the effect but also providing a reference for judging intensity differences between the two squares of the outer grid. (4) Number of diamonds: a larger set of diamonds produces a stronger perceptual effect. (5) Contrast between the 45° rotated outermost and innermost squares: reduced contrast weakens the effect, whereas high contrast reinforces it. Figure 3 shows the phenomenon at its full strength, created with a gray background, in which inverting or removing the markers markedly weakens the illusion.

When the Aquarius Starburst – Variant A is transformed into a gradient, it becomes equivalent to Vasarely's Nested Squares, a well-known Op Art illusion created by Victor Vasarely (Vasarely & Joray, 1970). In The Oxford Compendium of Visual Illusions, Martinez-Conde and Macknik analyzed Vasarely's Nested Squares alongside the Alternating-Brightness Star Illusion (Martinez-Conde & Macknik, 2017), showing that corners, angles, and line terminations strongly shape perceived brightness and salience. Related phenomena include the

Citation: Journal of Illusion 2026, **6**: 13831 - https://doi.org/10.47691/joi.v6.13831

Illusory-Streaks-from-Corners, first described by Roncato et al. (2016), in which diagonally oriented phantom lines appear to radiate from sharp corners and visually link neighboring figures despite the absence of physical contours.

Ellipse illusion and contrast-enhanced ellipse illusion

To further investigate the ray-beam effect, this article examines an illusion referred to as the ellipse illusion (Fig. 4, left). The first notable effect arises when two ellipses are placed vertically on top of each other, producing a pronounced lightness illusion at the major-axis vertices.

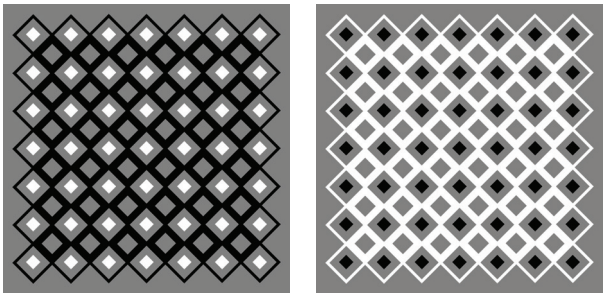

Fig. 3. Aquarius Starburst – Variant A: The GIF shows that the illusion is enhanced by contrast. The illusions resemble the earliest version, discovered incidentally and published in a Twitter post, now known as X (Capoot, 2023; Flaieh, 2019).

Despite constant luminance, this region appears lighter or darker than the surrounding field. A second effect emerges from the symmetrical positioning of pairs of vertically aligned ellipses, whose narrow contact zone is placed in proximity, thereby generating illusory contours. This illusion is comparable to the glare illusion, a gradient variant first described by Zavagno (1999), and some modifications of Scintillation-Starburst examined by Gianni Sarcone (2021).

Figure 4, middle and right, introduces a new variant of the ellipse illusion, named the contrast-enhanced ellipse illusion. This variant shows that the illusory effect is amplified when small polarity-inverted markers (45° rotated squares) are placed adjacent to the narrow gap between two ellipses on a gray background. The white markers strengthen the black ellipses' light illusory contours, while black markers strengthen the white ellipses' dark illusory contours. This amplification can be regarded as the third effect. Taken together, these three effects can be summarized as a lightness–contour–contrast interaction, characteristic of this illusion yet also present in other Starburst illusions.

Aquarius Starburst illusion – Variant B

Figure 5 shows that nearby arranged rhombuses of identical polarity can evoke three conditions: (1) Black rhombuses induce horizontally oriented dark rays in the gray region outside their short diagonals, whereas white rhombuses induce light ones (Fig. 5, panel 1). (2) White rhombuses

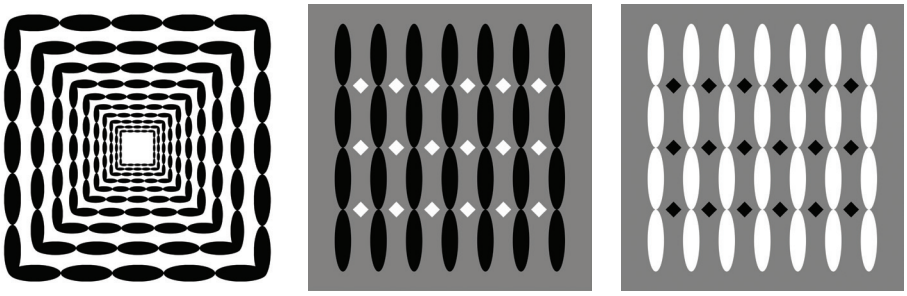

Fig. 4. Left: Ellipse illusion, middle and right: contrast-enhanced ellipse illusion. These demonstrations were first published in posts on X (Flaieh, 2025b, 2025c).

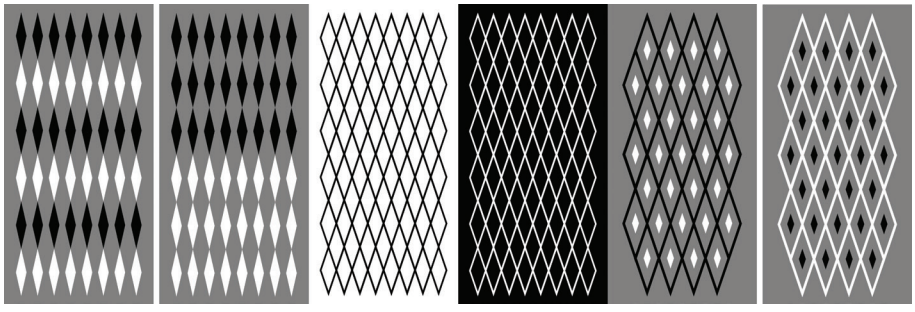

Fig. 5. Change in lightness in rhombuses and grids.

become lighter inside their short diagonals, whereas black rhombuses become darker (Fig. 5, panel 1). (3) When two rows of rhombuses with identical polarity are stacked, the tip between two black rhombuses lightens, whereas white rhombuses produce a dark one (Fig. 5, panel 2). This indicates that rhombuses can induce illusory lightness that varies depending on their relative luminance and fill density, which changes with respect to their width at different heights. The illusion becomes strong when the small inducing markers and the outer grid or ellipses produce the same lightness signal despite having opposite polarity, as in the Aquarius Starburst – Variant A (Fig. 3) and the Contrast-Enhanced Ellipse Illusion (Fig. 4, middle and right).

In both the Aquarius Starburst – Variant A and the contrast-enhanced ellipse illusion, white filled squares in diagonal orientation send light illusory signals through their corners, and black filled markers send dark illusory signals through their corners. An identical signal is sent from the grid vertices and the ellipses' major-axis vertices despite having opposite polarity relative to the markers, and when the signal matches, the effect becomes profound. Because the small marker in the Aquarius Starburst – Variant A has diagonals of equal length, it produces the same lightness signal at all four corners. As a result, the ray-beam effect becomes bidirectional, whereas compressing the grid makes it unidirectional (Fig. 5, panels 5–6) because the lightness signals no longer match across all directions. The same condition appears in the Spinnwebfäden illusion (Prandtl, 1927): a grid of 45° rotated squares yields a bidirectional ray-beam effect, whereas compressing the grid into rhombuses favors a unidirectional one, with black grids producing light contours and white grids producing dark ones, similarly to Motokawa's rhombuses (Motokawa, 1950) (Fig. 5, panels 3 and 4). In those cases, the ray-beam direction aligns with the shortest diagonal of the rhombuses.

The Aquarius Starburst – Variant B (Fig. 6) is created by following three core principles: (1) Considerations of the lightness distribution in rhombuses, in which markers with identical fill density, shape, and lightness effects are matched with each other. When the short and long diagonals of the rhombuses are identical, they are transformed into 45°-rotated squares, in which corners of filled white squares induce light contours in all four directions, while corners of filled black squares induce dark ones. Figure 6 shows that the grid's lightness can be altered by adding filled, 45°-rotated inner squares of identical polarity at its vertices, together with a same-polarity inducer at the center, which reverses the lightness effect and makes the white grid appear lighter and the black grid darker. (2) The linear organization of black, 45°-rotated filled squares with identical corners and orientation enhances the formation of dark contours, whereas linear organization of white, 45°-rotated filled squares with identical corners and orientation enhances the formation of light contours. (3) Contrast combinations with markers of different sizes induce contours of opposite intensity that extend from the corners of the 45°-rotated squares, which disrupt lightness estimation and elicit scintillations (Fig. 6, gif). This type of contrast combination also shrinks the lightness effect into a narrower thread, as in the Orion Starburst – Variant A (discussed later), which becomes noticeable when the illusion is compressed horizontally or vertically to examine lightness interference in different directions of the squares.

Figure 7 (left) shows that removing the two small squares positioned at the corners along either principal axis of the outermost hollow square makes the ray-beam effect unidirectional. The resulting basic element produces a dominant axis aligned with the two remaining small squares, which exhibit markedly higher lightness intensity than the unoccupied axis. The illusion is most easily seen when the central space between every four vertically oriented basic elements contains one horizontally oriented basic element and vice versa. By adding gray borders around the element, the illusion is strengthened through the interaction between the small squares and the opposite-polarity background vertices, comparable to the Aquarius Starburst – Variant A. Figure 7 (right) uses an identical configuration and is created by removing the central inducer while enlarging the two added squares at the vertices until they meet with minimal contact. This procedure creates two small light squares that should be positioned as closely as possible to induce a strong effect. Each basic element generates a unidirectional contour, whereas the final alternating configuration

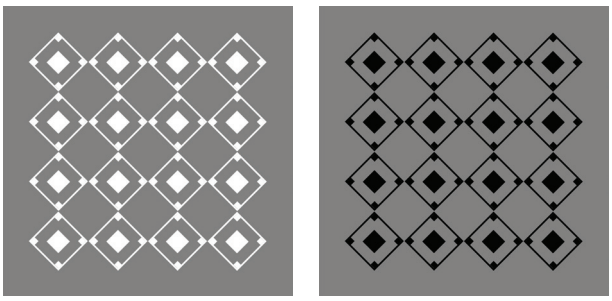

Fig. 6. Aquarius Starburst – Variant B.

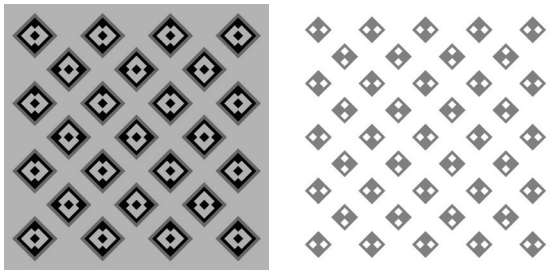

Fig. 7. Unidirectional ray-beam effect in the Aquarius Starburst – Variant B.

Citation: Journal of Illusion 2026, **6**: 13831 - https://doi.org/10.47691/joi.v6.13831

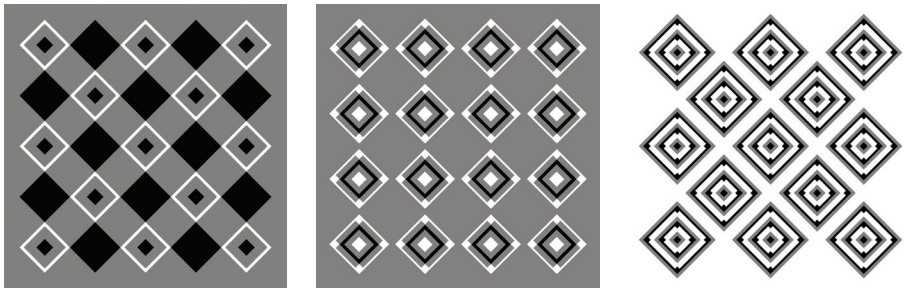

Fig. 8. Combination of the Aquarius Starburst – Variants A and B.

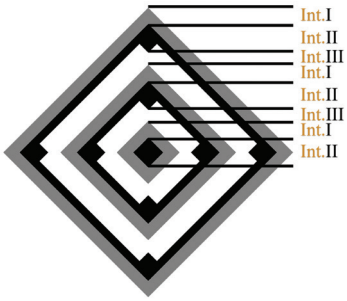

Fig. 9. Three interaction types: I. Opposite-polarity int. II. Intrinsic square signal. III. Same-polarity int.

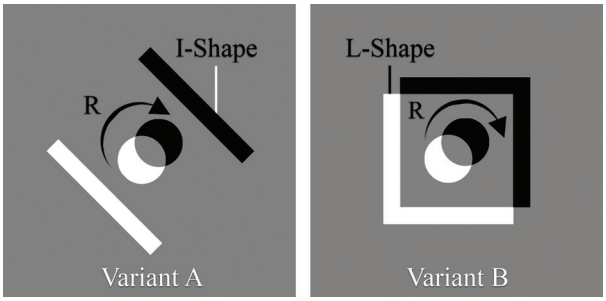

Fig. 10. Basic elements in the Pisces Starburst illusion – Variant A on the left and Variant B on the right. R: Rotatable.

combines horizontally and vertically oriented elements, thereby potentiating the visibility of the illusion.

Figure 8 is obtained by combining the Aquarius Starburst – Variants A and B. When the basic element of Variant A is attached corner-to-corner to a filled, 45° rotated square that induces identical lightness signals in all four directions, the illusion is enhanced (Fig. 8, left). The combination of Variants A and B in Fig. 8 (middle and right) is arranged corner-to-corner or in close adjacency to prevent disrupted, non-identical polarity-based lightness signals from arising where the two variants meet.

Figure 8 (right) evokes illusory contours through three types of interaction: (1) an opposite-polarity interaction, generated by the lightness signal between the small squares and the vertices of opposite polarity, as in the Aquarius Starburst – Variant A; (2) an intrinsic square signal, produced within the small squares; and (3) a same-polarity interaction, arising from the lightness signal between the small squares and the gray vertices, which share the same contrast-polarity sign, as in the Aquarius Starburst – Variant B. Figure 9 shows where these interactions are localized within the basic element, which sends identical lightness signals in all directions.

Pisces Starburst illusion – Variant A

When (1) two layers of the Aquarius Starburst – Variant A (Fig. 2) with opposite polarity on a gray background (2) are superimposed, (3) combined using 50% additive alpha blending, and (4) the foreground layer is displaced horizontally, vertically, or both, these four operations, depending on the displacement direction, yield two novel variants, Pisces A and B. Replacement of the small markers with two overlapping circles, with a gray region at their intersection, produces Fig. 10, which evokes a pronounced ray-beam effect while also generating a strong lightness illusion.

This illusion conveys the impression of two fish swimming in opposite directions, inspiring the name 'Pisces' in reference to one of the 88 official constellations defined by the International Astronomical Union (IAU) (Delporte, 1930). The full designation is therefore the 'Pisces Starburst Illusion'. Variant A of the Pisces Starburst arises when the configuration consists of two 45° I-shaped bars of opposite polarity, together with a small pair of overlapping circles whose polarities match the adjacent bars and whose shared diagonal axis aligns with the bars' orientation. The adjustable element is the pair of small markers, which can be substituted or freely rotated to modulate the strength of the illusion. Figure 10 shows the standard configuration (SC) without any additional marker adjustments, which evokes the maximal effect.

Figure 11 (left) demonstrates Variant A, which induces two different effects: illusory lightness and illusory contours that run along segment terminations of the same contrast polarity. The middle panel demonstrates that the illusion persists even when the basic element is rotated

horizontally. The right panel illustrates a polar-coordinate transformation, where the opacity of the I-shaped bars is reduced by 50% against a neutral-gray background to create a pleasant effect without disrupting the outcome. The ray-beam effect in the right panel produces a mirrored spiral pattern – a geometric illusion whose direction is ambiguous and may reverse bidirectionally. The GIF in Fig. 11 illustrates that both the inner markers and the I-shaped bars are essential for a strong activation of the illusion; removing either component causes the illusion to fade or lose coherence.

The markers can be substituted with different shapes – such as overlapping circles, spaced lines, or hearts – without disrupting the illusion, whereas the outermost I-shaped bars are harder to replace. Figure 12 (left) presents the inner-lines variant, exhibiting illusory lightness and contours that extend bidirectionally from the line terminations. The middle panel demonstrates the line-based gingham configuration, obtained by mirroring the basic elements of the line version, which reveals an illusory cross along the horizontal and vertical axes that evoke a transparency effect. The figure (right) is obtained by manipulating the polarity of the middle panel and shows margins that form illusory squares. The gif further reveals that the illusion fades when the lines are entirely black or white and remerges when they contain a mixture of both, indicating that contrast contributes to the appearance of the illusion. The middle and right configurations (Fig. 12) can exhibit weak scintillations in the central gap, particularly when the lines are uniformly black or white, like the Ehrenstein illusion (Ehrenstein, 1941).

Figure 13 shows that the lower white and upper black elements can each generate an illusory margin on their own, which resembles a right triangle. Figure 12 (left), which uses the same configuration, demonstrates that the contour disappears when both the lower and upper elements share the same luminance – whether both become white or both become black – and the perceptual discrimination drops. Together, these findings indicate that contrast allows light and dark illusory contours to coexist. The contrast also induces a secondary effect – illusory lightness – that aligns with the direction of the contours and adds new details that make the contours more visible and recognizable. This combined effect can be described as contrast-based lightness–contour coactivation.

When the Pisces Starburst – Variant A is rotated to 45°, its shape becomes structurally similar to the Long-Range Argyles (LoRAs) illusion, in which two opposite-polarity triangles meet at their right angles, although LoRAs lack gaps inside the basic element. LoRAs produce strong lightness-contrast, as shown by Flynn and Shapiro (2014), in which the gray background appears lighter against dark triangles and darker against light ones. By fulfilling certain conditions, the Pisces Starburst – Variant A is also evoking lightness contrast. Figure 14 (left) is generated by vertically repeating the basic elements and adding a mirrored copy. The lightness contrast becomes visible by: (1) increasing

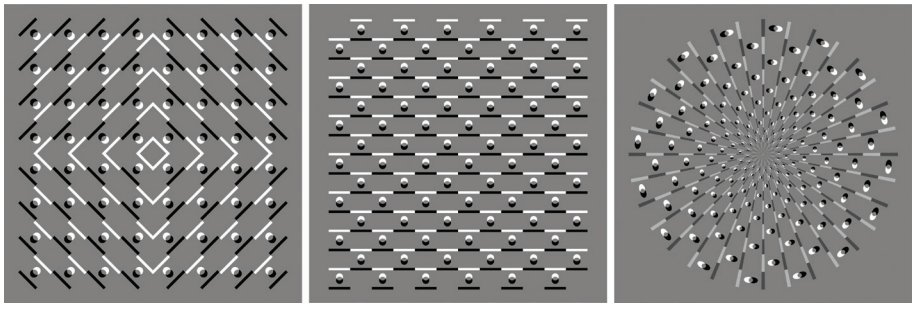

Fig. 11. Pisces Starburst – Variant A. Earlier variants of the middle and right illusions were published on X (Flaieh, 2025d, 2025e).

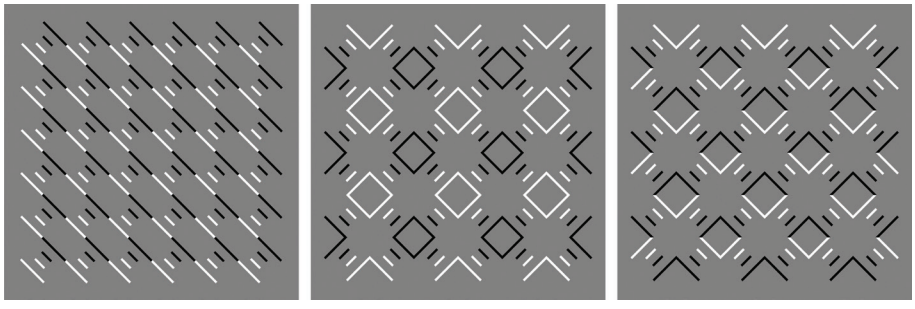

Fig. 12. Pisces Starburst – Variant A (inner lines version).

Citation: Journal of Illusion 2026, **6**: 13831 - https://doi.org/10.47691/joi.v6.13831

the quantity of the basic element, (2) when the illusion is viewed from farther away, and (3) with vertical shaking. (4) When either the innermost markers or the outer bars are removed at long viewing distances, the stimulus induces lightness assimilation; therefore, both the inner and outer lines are necessary for the formation of lightness contrast. If at least some of these conditions are not met, lightness contrast becomes difficult to perceive and instead shifts toward long-range lightness assimilation (Fig. 14, middle). When the Pisces Starburst – Variant A is placed vertically with a spatial separation, without the arrangement that usually induces the strong lightness-contrast effect, the illusion can still exhibit long-range contour formation. This formation is extended by the line terminations, as in the Ehrenstein illusion (Ehrenstein, 1941), and is driven by contrast-based lightness–contour coactivation (Fig. 14, right), in which the addition of a diffuse lightness effect enhances the illusion.

Figure 15 (left) shows Variant A, consisting of diagonal bars with identical slopes (45°) and a vertical red line passing through their midpoint as a reference boundary. When the bars are rotated to a horizontal orientation, they become parallel – white bars on the left and black bars on the right. Thereafter, by reducing the configuration to a single black–white pair, strong lightness assimilation occurs (Fig. 15, right), without shifting to lightness contrast through spatial distance or vertical shaking. The middle panel shows the transition from Variant A – Line Version to the straight-line arrangement. The illusion reaches its peak in the Pisces Starburst state, where stable illusory contours and lightness contrast are present, but it weakens – without disappearing – when the configuration shifts toward horizontal lines, which exhibit lightness assimilation. The loss in strength compared to the right panel indicates that line spacing and spatial frequency modulate the magnitude of lightness assimilation. These observations show

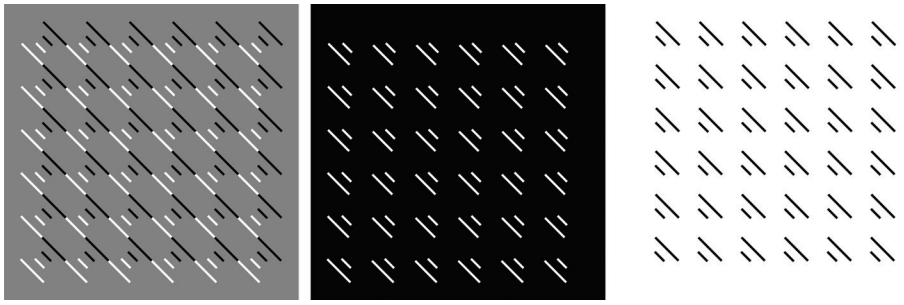

Fig. 13. Contrast-based lightness–contour coactivation.

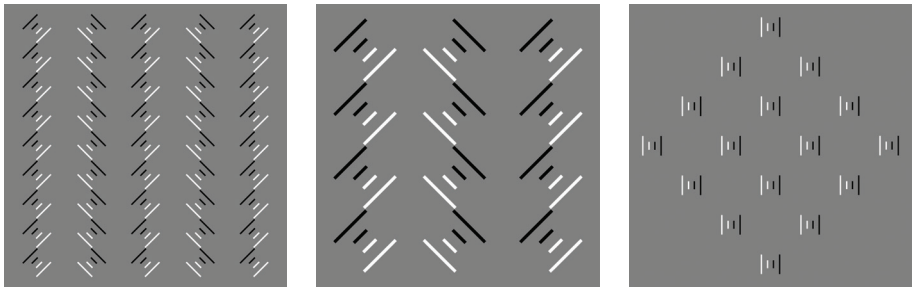

Fig. 14. Left: Lightness contrast induced by increased element quantity and size reduction. Middle: The illusion is perceived as lightness assimilation up close. Right: Long-range contour formation.

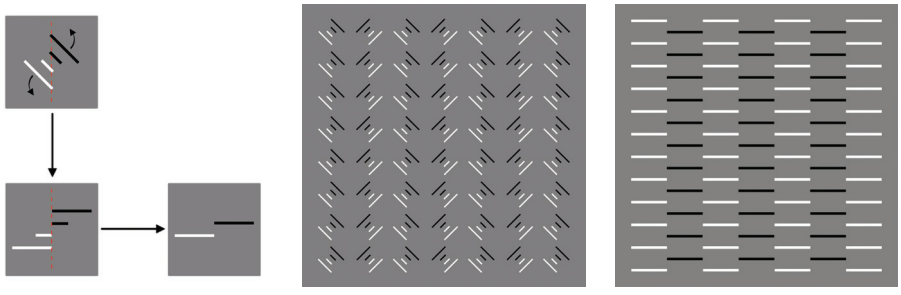

Fig. 15. Transformation of the Pisces Starburst – Variant A into a straight-lines arrangement.

that the Pisces Starburst – Variant A – due to its structural similarity to the right triangles in LoRAs (Flynn & Shapiro, 2014) – evokes lightness contrast, while variations in line angle and length modulate induction, with identical length favoring assimilation and shifting the illusory margin from bidirectional to unidirectional.

Figure 16 (right) uses heart-shaped inner markers that can replace the original elements while preserving a similar effect with a different intensity. The illusion weakens when only the hearts are present and disappears when only the lines remain. With both elements present, it produces illusory scintillation, lightness transparency, and contours. Figures 12 (middle) and 16 (right) show configurational similarities to the gingham illusion (Tyler, 2000), which can evoke both scintillation and illusory transparency. The original gingham transparency illusion, which corresponds to a cross shape, is shown on the left side of Fig. 16. The two adjacent panels display similar transparency effects generated by overlapping shapes with a progressively increasing number of corners. The gray region marked with a plus sign alternates between appearing as a lighter or darker transparent layer, depending on eye blinks or shifts in perceptual mindset. The illusions in the left row are created by (1) overlapping a black and a white geometric shape against a 50% gray background, (2) adjusting the opacity of the black and white to 50% to create a mid-gray intersection via the opacity function in a raster-graphics program, and (3) using symmetric organization to induce a trap that interferes with lightness-contrast estimation.

Pisces Starburst illusion – Variant B

The Pisces Starburst Illusion – Variant B arises when the configuration consists of two outermost orthogonal L-shaped bars of opposite polarity, combined with two overlapping inner circles of opposite polarity and an elliptical neutral-gray region at their intersection. The two overlapping innermost markers are an adjustable element that can be freely rotated to modulate the strength of the illusion. Figures 10 and 17 illustrate the SC, in which the orientation and polarity of the inner markers align with the adjacent L-shaped bars, which induces two main effects: illusory contours and lightness.

A lightness-assimilation effect appears inside the basic element on a uniform gray background: the neutral gray (L = 50%) looks lighter when surrounded by white markers and L-shaped bars (area A in Fig. 18, right) and darker where surrounded by black ones (area B in Fig. 18, right). This lightness effect appears when two basic elements are mirror-reversed, meaning that they are flipped horizontally or vertically to create clear geometric symmetry (Fig. 18, left). Furthermore, a contiguous configuration (Fig. 18, middle) is necessary to strengthen lightness assimilation, whereas the effect shifts to lightness contrast in a noncontiguous cross configuration, in which the lightness contrast appears in the central gap between the basic elements (area C in Fig. 18, right). A contiguous configuration is a unified arrangement in which some elements of identical polarity meet edge-to-edge. Figures 17 and 18 (middle) show three optimal variants:

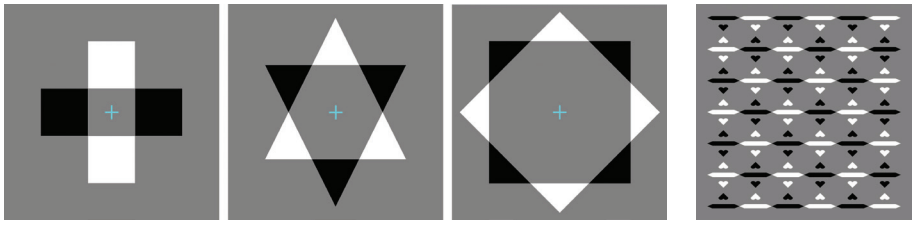

Fig. 16. Left: Gingham illusion and similar figures that evoke a transparency effect, which becomes more noticeable when the configuration is repeatedly inverted. Right: The Innermost Hearts version evokes transparency through its structural similarity to the Gingham illusion. The illusion to the right was first published on X (Flaieh, 2024c).

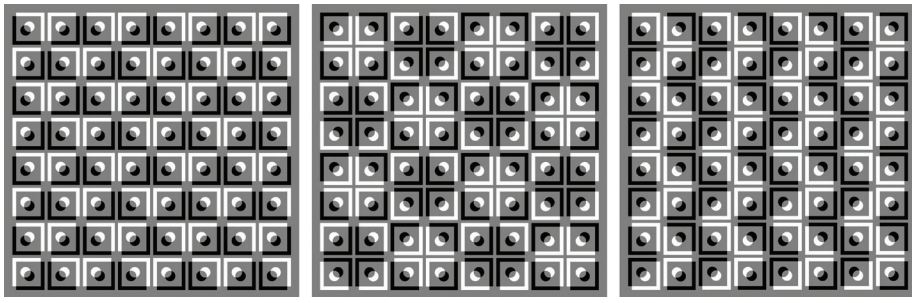

Fig. 17. The GIF shows that the innermost markers together with the outermost orthogonal bars are required to fully activate the illusion, which is supported by polarity unification. The illusions on the left and in the middle were first published on X (Flaieh, 2024a, 2024b).

Citation: Journal of Illusion 2026, **6**: 13831 - https://doi.org/10.47691/joi.v6.13831

(1) a mirror-inverted T-shape, (2) a cross shape, and (3) an inverted T-shape, where each one can yield two variations of opposite polarity. A noncontiguous cross configuration (Fig. 18, right) is formed by rearranging the basic elements into a discrete, cross-like layout in which the L-shaped bars of identical polarity meet corner-to-corner, inducing lightness contrast. If the corners are paired with basic elements of opposite-polarity, causing the lightness contrast in the central gray region to fade, this configuration is termed a noncontiguous SC (Fig. 19, left).

The Pisces Starburst – Variant B produces a diagonally oriented, unidirectional ray-beam effect (Fig. 19), corresponding to the combination of illusory lightness and contours, whereas Variant A exhibits a bidirectional one (Fig. 11, right). A range of orientations can be obtained in Variant B by organizing the basic elements (Fig. 17) into new configurations. Among the other illusions discussed earlier, the Aquarius Starburst Variants A-B (Figs. 3 and 6) produce bidirectional ray-beam effects, whereas the Contrast-Enhanced Ellipse (Fig. 4, middle and right) yields a unidirectional one. These illusory ray-beam effects can also generate geometrical illusions (Figs. 11, right, and 19, right). When Variant B, in a noncontiguous SC – meaning without directional adjustments – is converted to polar coordinates, its unidirectional ray-beam effect generates an illusory spiral. If the polarity between the innermost markers and the outermost bars is not unified, the spiral breaks (Fig. 19, right) because the total spatial coherence of the image reduces or becomes diffuse.

The spiral is supported by the diagonal L-shaped outermost bars but becomes visible when the inner marker with identical orientation reinforces unification and restores structural coherence through polarity matching, a similar condition also occurring in Variant A (Fig. 11, right). The strength of the SC shows that the unification (grouping) of perceptual elements with the same contrast polarity enhances the formation of illusory contours (Figs. 17 and 19, right, gif). This is consistent with Roncato's (2017) description in The Oxford Compendium of Visual Illusions, which shows that the visual system preserves luminance-contrast polarity during completion, and that polarity mismatches interfere with the polarity-dependent completion that supports extended contour integration.

Figure 20 (left) shows the Pisces Starburst – Variant A – the terminal-point version, where the illusory margin persists when the inner lines are replaced by small squares with correct polarity at their terminations while leaving the outer bars intact. Figure 20 (right) presents the Pisces Starburst – Variant B innermost-clamps version, showing that the illusory contours persist when the outermost bars are thinned, and only the clamps intersecting the two markers are retained. The innermost parts contain a pair of small squares with opposite polarity placed at the two points of intersection. The result shows that the margin is illusory rather than physical and emerges when the inner marker's terminal point (Variant A) or the clamp intersection (Variant B) connects to the line terminations of the outermost bars. In both variants, markers with identical polarity must share the orientation of the outer bars of identical polarity, influencing perceptual unification and the perceived direction of the ray-beam.

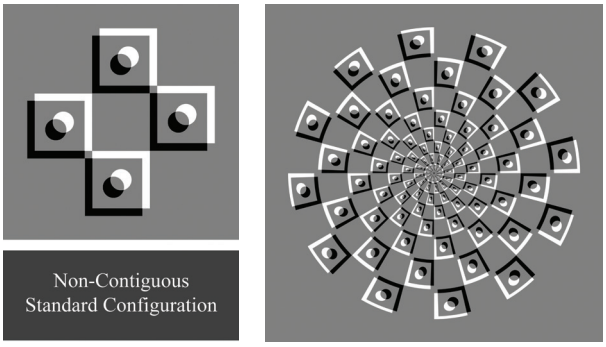

Fig. 19. Left: A noncontiguous standard configuration. Right: Spiral formation via diffuse change in lightness and contour completion supported by polarity unification.

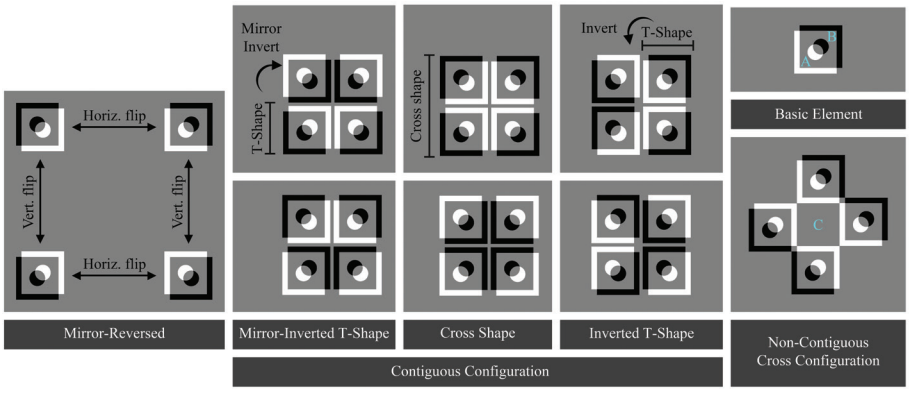

Fig. 18. Different arrangements in the Pisces Starburst – Variant B.

The L-shaped bars of opposite polarity, in the absence of the central inducer, can give rise to three distinct illusory phenomena:

(1) The orthogonal L-shaped bars of opposite polarity correspond to the basic element of the Pinna–Brelstaff illusion (Pinna & Brelstaff, 2000), a visual pattern known to elicit an illusion of relative motion. A similar effect appears in the inverted T-shape (Fig. 17, right) when viewed up close, where slow vertical displacement of the mouse pointer induces a motion illusion, while this effect is blocked in the mirror-inverted T-shape and in the cross shape.

(2) Figure 21 (left) shows that when the mirror-inverted T-shape is turned vertically, the perceived depth changes, while this effect weakens when the central inducer is removed. This illusory effect can be observed in a single basic element and becomes more pronounced in the mirror-inverted T-shape configuration. A similar phenomenon appears in Fig. 12 (right) when the pattern is turned vertically, in which the change in depth is mainly induced by the opposite-polarity L-shaped bars. Figure 21 (right) shows that replacing the illusory contours and lightness in the mirror-inverted T-shape with real surfaces of matching luminance makes the illusory depth even stronger, which becomes noticeable when the final pattern is turned vertically. The depth illusion appears as either convex or concave and is strongest when both the L-shaped bars and the innermost marker remain intact, yet it stays robust even if one of these two elements is removed. This illusion resembles Ramachandran's crater illusion, which governs shape-from-shading interpretations and follows the visual system's light-from-above prior – the assumption that illumination typically comes from above – leading to a reinterpretation when the diamonds are turned vertically (Ramachandran, 1988). The demonstration shows that the L-shaped bars, together with an explicit representation of the illusory contour and the lightness effect strengthened by the central inducer, enhance the depth effect in the mirror-inverted T-shape. Among the other illusions in this article, the Aquarius Starburst – Variant A changes depth via shape-from-shading both concavely and convexly, whereas the Orion Starburst – Variant B produces a similar effect mainly driven by its U-shape.

(3) The diagonal separating the two L-shaped bars of opposite polarity in the contiguous cross shape (Fig. 17, middle) can also divide areas with different grayness. A faint dark shadow emerges in the gray region enclosed by the black L-shaped bars, whereas a faint light shadow appears in the gray region enclosed by the white ones. This lightness induction becomes notable when L-shaped bars of opposite polarity are combined and demonstrates that a weak lightness illusion can arise even without the central inducer. The illusion becomes easier to observe from a distance and in peripheral vision. The addition of the central inducer enhances the discriminability of the diffuse lightness effect produced by the L-shaped bars and facilitates the emergence of illusory contours.

Figure 22 (left) was generated by decomposing the element with identical polarity from the cross-shaped contiguous configuration, which exhibits partial similarities to Schumann's contour illusion (Schumann, 1904), in which illusory squares are formed in the neutral-gray area, while yielding a weak lightness effect due to lack of contrast. The Pisces Starburst – Variant B exhibits a stronger effect when elements of opposite polarity are combined, revealing contrast-based lightness–contour coactivation. The middle and right panels show a split form of the Aquarius Starburst – Variant A of opposite polarity, which in

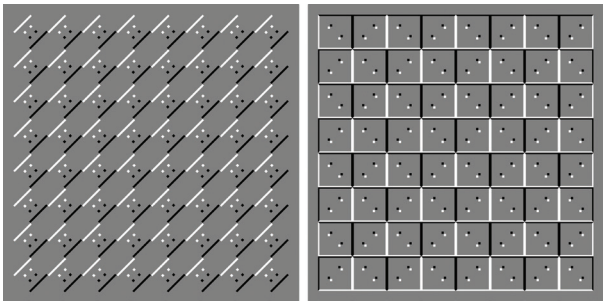

Fig. 20. On the left: Pisces Starburst – Variant A terminal-point version; on the right: Pisces Starburst – Variant B innermost-clamps version. In both images, illusory contours dominate while the lightness effect weakens compared with the standard variant.

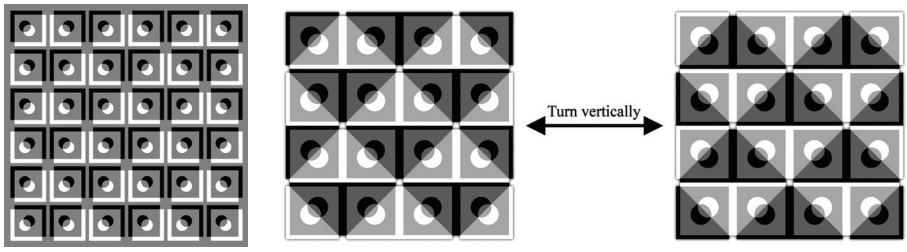

Fig. 21. Left: Emergence of shape-from-shading via vertical turn of mirror-inverted T-shape. Right: Replacing the illusory contour and lightness with real, luminance-matched surfaces makes the depth impression stronger. A similar illusion to the right was first published on X (Flaieh, 2025a).

Citation: Journal of Illusion 2026, **6**: 13831 - https://doi.org/10.47691/joi.v6.13831

combination produces the Pisces Starburst – Variant B. The middle panel shows a diagonal illusory margin that passes through the white innermost markers and the terminations of the black outer L-shaped bars, with the side containing the white markers appearing lighter and the interiors of the black bars appearing darker. The right panel shows the complementary elements: a diagonal illusory margin that passes through the black innermost markers and the terminations of the white outer L-shaped bars. The side containing the black inner markers appears darker, while the interiors of the white L-shaped bars appear lighter. In both the middle and right demonstrations, an illusory diamond emerges, which is obtained by organizing the element continuously along the same diagonal. In the complete Aquarius Starburst – Variant A composed of two identical split forms, the vertex in the grid emanates a thin illusory lightness, while the innermost marker sends an identical lightness signal from its corners, consistent with the markers' relative luminance. A linear and diagonal arrangement comparable to Fig. 22, middle and right, is created in a complete contiguous configuration, which evokes lightness assimilation inside the L-shaped bars and simplifies contour formation by grouping elements of identical polarity. This linear arrangement can also cause the ray-beam effect to extend in multiple directions while maintaining coherence.

Lightness assimilation refers to a perceptual shift in which a region's apparent lightness moves toward the luminance of adjacent elements. Figure 23 illustrates three configurations that preserve both color and lightness assimilation, each clarifying the underlying mechanism. Figure 23 (left) shows that the illusory effect in the Pisces Starburst – Variant B persists in color and requires both dark and light components to be sustained. Figure 23 (middle) shows a solid version of the Craik–O'Brien–Cornsweet illusion (Cornsweet, 1970), created by replacing the gradient with uniform color through a color-reduction function in a raster editor. This demonstration shows that two factors are required for assimilation to occur. The first is polarity-matching enclosure, in which lightness assimilation arises when a neutral-gray region lies between two lines of the same color or luminance (yellow–gray–yellow, blue–gray–blue, black–gray–black, or white–gray–white), causing the gray region to be perceptually drawn toward the color or lightness of the enclosing lines. The second requirement is contrast-pair adjacency, which is necessary for strong activation of the assimilation effect and requires that the adjacent lines be complementary colors or form clear contrast pairs, such as blue next to yellow or black next to white. A similar polarity ordering and arrangement can be found within a single basic element of the Pisces Starburst Illusion and the Orion Starburst Illusion. These two requirements are also crucial in the watercolor illusion, which induces color spreading and assimilation (Pinna et al., 2001) and is composed of wavy contours that enable long-range interactions. Figure 23 (left and right) shows that higher spatial frequency can also induce assimilation. This means that the lines of identical polarity in

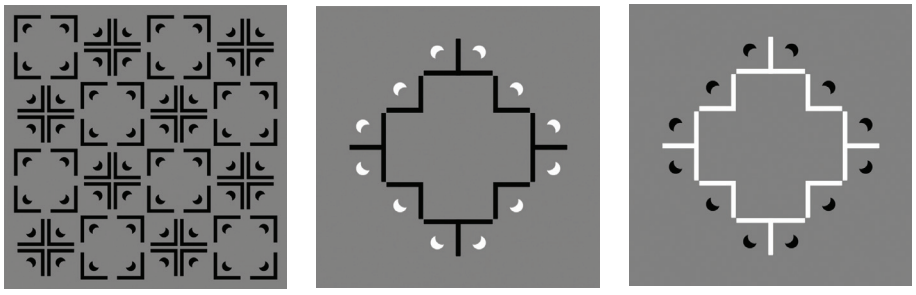

Fig. 22. Left: Decomposition of the contiguous cross configuration. Middle and right: The split form of the Aquarius Starburst – Variant A.

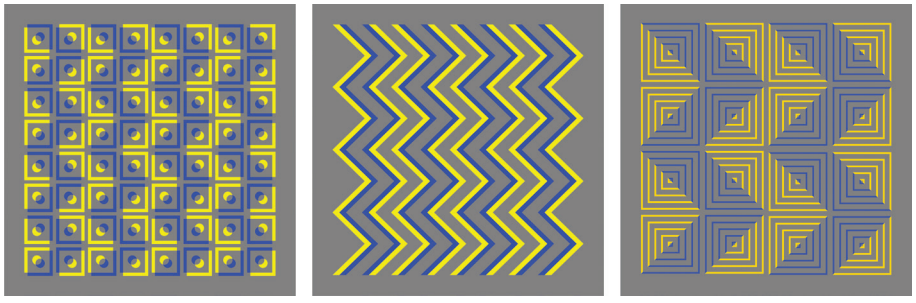

Fig. 23. Three color assimilation illusions are shown and then displayed in Luminosity mode. The GIF demonstrates that polarity-matching enclosure, contrast-pair adjacency, and spatial frequency strengthen the assimilation effect.

front of the neutral-gray region must be numerous, dense, and regular. The contiguous configuration yields stronger assimilation by maintaining favorable polarity ordering and spatial frequency that sustains a constant lightness assimilation. However, spatial frequency alone produces weaker lightness assimilation, whereas contrast differences are crucial for potentiating the effect and are also essential to discriminate the change in lightness. The basic element in Fig. 23 (right) evokes a bidirectional ray-beam effect, in which corners of identical polarity with high spatial frequency generate vibrant illusory contours. In the Pisces Starburst – Variant B, the circular shape and the configurational organization reduce contour formation with vertices of identical polarity, causing the contour to emerge in a single direction while maintaining higher spatial frequency through the contiguous configuration.

The illusion in Fig. 24 is constructed by drawing a diagonal boundary contour that divides the L-shaped bars into two complementary regions, black on one side and white on the other. Along this diagonal contact line, the L-shaped bars are arranged corner-to-corner so that the endpoint of each black L-shaped bar touches the adjacent white one. This arrangement induces a strong lightness contrast in the gray region between the two L-shaped bars of identical polarity, comparable to the Koffka ring illusion and Adelson's ring illusion (Adelson, 2000; Koffka, 1935). The neutral-gray areas A and B appear lighter when surrounded by black L-shaped bars, whereas area C appears darker when surrounded by white L-shaped bars.

To avoid the occurrence of lightness contrast, the gray zone at the diagonal boundary inside the basic element of the Pisces Starburst – Variant B should not be blocked. A single basic element lacks the arrangement shown in Fig. 24 and produces a diffuse change in lightness, which appears as strong lightness assimilation when arranged in a contiguous configuration. The interaction between the basic elements in the Pisces Starburst – Variant B can, under certain circumstances, lead to lightness contrast, as in a non-contiguous configuration. Figures 25 and 26 indicate that even within a contiguous configuration, different layers – based on their specific geometrical shapes – can elicit lightness contrast; yet, when all layers are perceived as a unified structure, lightness assimilation remains functional.

The mirror-inverted T-shape can be decomposed into four complementary layers in which L-shaped corners of opposite polarity meet at their right angles (Fig. 25, left). Each configuration resembles a long-range Argyle arrangement that produces lightness contrast. The similarities become most apparent when the L-shaped bars are paired with identical-polarity innermost markers, thereby promoting favorable contour integration and producing an appearance comparable to the Long-Range Argyle illusion. The lightness contrast increases in intensity (1) when the pattern is viewed from a sufficient distance;

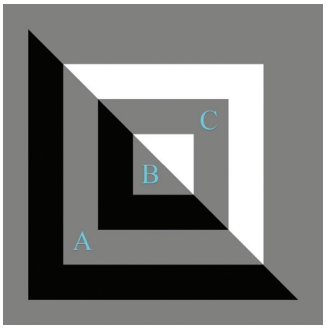

Fig. 24. Area A = B = C = 50% gray. First published on X (Flaieh, 2024d).

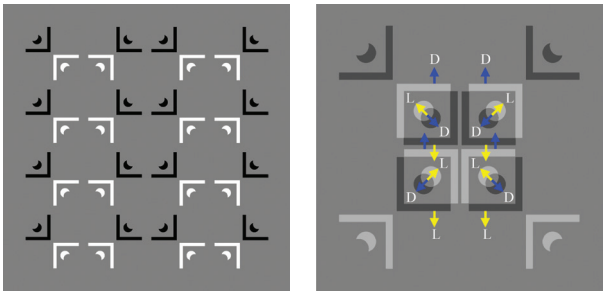

Fig. 25. Left: The decomposition of the mirror-inverted T-shape reveals structures that elicit lightness contrast, yet together they induce lightness assimilation. Right: Interactions between the basic elements in the mirror-inverted T-shape: D = darken, L = lighten; yellow arrow: region lightened by lightness contrast; blue arrow: region darkened by lightness contrast.

(2) when the number of elements is increased; or (3) by subtle vertical shaking. If all four layers are combined, the induced lightness contrast does not disrupt the lightness assimilation; the black segments fall into gray regions already shifted toward a darker appearance, and the white segment into regions shifted toward a lighter one (Fig. 25, right). In the Pisces Starburst – Variant B, four basic elements can form a contiguous configuration that supports lightness assimilation. However, this configuration cannot be applied to the Long-Range Argyle units, which do not permit polarity-matching enclosure, meaning that the illusion requires a neutral-gray region between two segments with identical luminance to allow lightness induction to pass through.

A similar effect appears in the uniform cross shape in Fig. 26 (left) and in the inverted T-shape in Fig. 26 (right), which can be described as follows: (1) The white L-shaped bars and the innermost markers of identical polarity darken the surrounding gray area through lightness contrast, whereas the black L-shaped bars and innermost markers of identical polarity lighten it. (2) Organizationally, white elements of the complementary layer are placed in the gray regions that lighten by lightness contrast via the primary layer, and the black elements of the

Citation: Journal of Illusion 2026, **6**: 13831 - https://doi.org/10.47691/joi.v6.13831

complementary layer are placed in the regions that darken by lightness contrast via the primary layer. (3) This arrangement matches the elements' relative luminance with the lightness induction (contrast) present at their location, which does not disrupt the lightness assimilation in which the gray area adjacent to black elements appears darker, and the gray area adjacent to the white elements appears lighter. This combined interaction can be described as the luminance-contrast convergence effect.

Figure 27 shows the progressive change in the opacity of the complementary layer in the uniform cross shape from 0 to 100%. At around 20%, it appears as if the induced contrast can easily pass through the complementary layer of lower opacity. The addition of new contours (20–100%), which have identical luminance to the induced lightness contrast in the same area, reinforces the changed lightness induction to become stronger. The higher the opacity, the more pronounced the strength of the illusion becomes. The complementary layer also induces a change in lightness that strengthens the lightness induction in the primary layer, which can be observed when the opacity levels at 0 and 100% are compared.

Figure 28 illustrates the decomposition of the contiguous cross shape, in which the addition of the L-shaped bars and the central inducer occur progressively. Panels 1B, 2B, 3B, and 4B correspond to the progressive addition of four equal zigzag patterns, which increase from left to right, identical to Fig. 29 on the left. Each new layer that is added can evoke new interactions in the surrounding areas. Panels 1A, 1B, 1C, 1D, 2C, 2D, 3A, 3B, and 3C exhibit lightness contrast in the empty gray area with varying intensity. Panels 1E, 2A, 2B, 4A, and 4B exhibit a transparency illusion with varying intensity, like the gingham

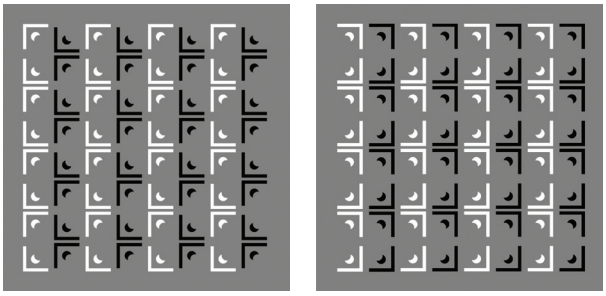

Fig. 26. Left: The uniform version of the cross shape. Right: Inverted T-shape.

illusion (Fig. 16). Panels 2, 3, and 4 show that lightness assimilation can occur inside the L-shaped bars regardless of the occurrence of either lightness contrast or transparency in the outer gray area. Panels 2C and 2D show the formation of a diagonally oriented dominant contrast axis in the empty gray area, which reduces the transparency illusion seen in panel 2B. A dominant concentration of white units with the correct angle darkens the gray area, whereas a dominant concentration of black units with the correct angle lightens the same area. This demonstration shows that, in the absence of L-shaped bars in some conditions, even the central inducer can evoke lightness contrast.

Panel 3B shows that when L-shaped bars are added to Panel 2D, the lightness contrast induced by Panel 2D will dominate outside the added L-shaped bars in the empty gray area. Panels 3B and 3C show that the empty gray area receives an induction identical to the luminance of the missing units, indicating that the luminance-contrast convergence occurs correctly in this region. The demonstration in Fig. 28 shows that the lightness estimation switches between lightness contrast and transparency when the illusion is incomplete, and that the result in panel 4B is influenced by the luminance-contrast convergence effect, which can be received as lightness assimilation. However, the central region between each four cross-shaped configurations (Panel 4B) contains both dark and light elements, generating conflicting lightness signals that allow the transparency illusion to persist even in the complete figure. The difference between the uniform cross shape (Fig. 27) and the cross shape (Fig. 28) is that the cross-shape alternates between two configurations of opposite polarity, which, in addition to lightness assimilation, can also produce a transparency effect.

Figure 29 (left) shows that splitting Pisces Starburst – Variant B at the midpoint and shifting the halves vertically produces the zigzag pattern. Pairing the outermost bars with identical-polarity innermost markers yields strong and sharp vertical contours. The illusion is strongly activated when two L-shaped bars of opposite polarity connect at their endpoints. When the pattern is arranged so that the L-shaped bars of identical polarity meet corner-to-corner, it can induce lightness contrast, as in Adelson's snake illusion (Adelson, 2000; Somers & Adelson, 1997). Four complementary layers of this zigzag pattern can be found by decomposing the cross shape (Fig. 28), which does not disrupt the lightness assimilation.

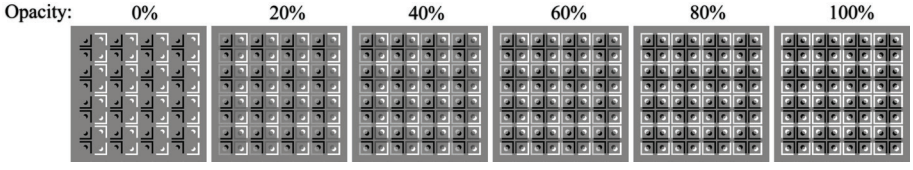

Fig. 27. A progressive change of the complementary layers' opacity.

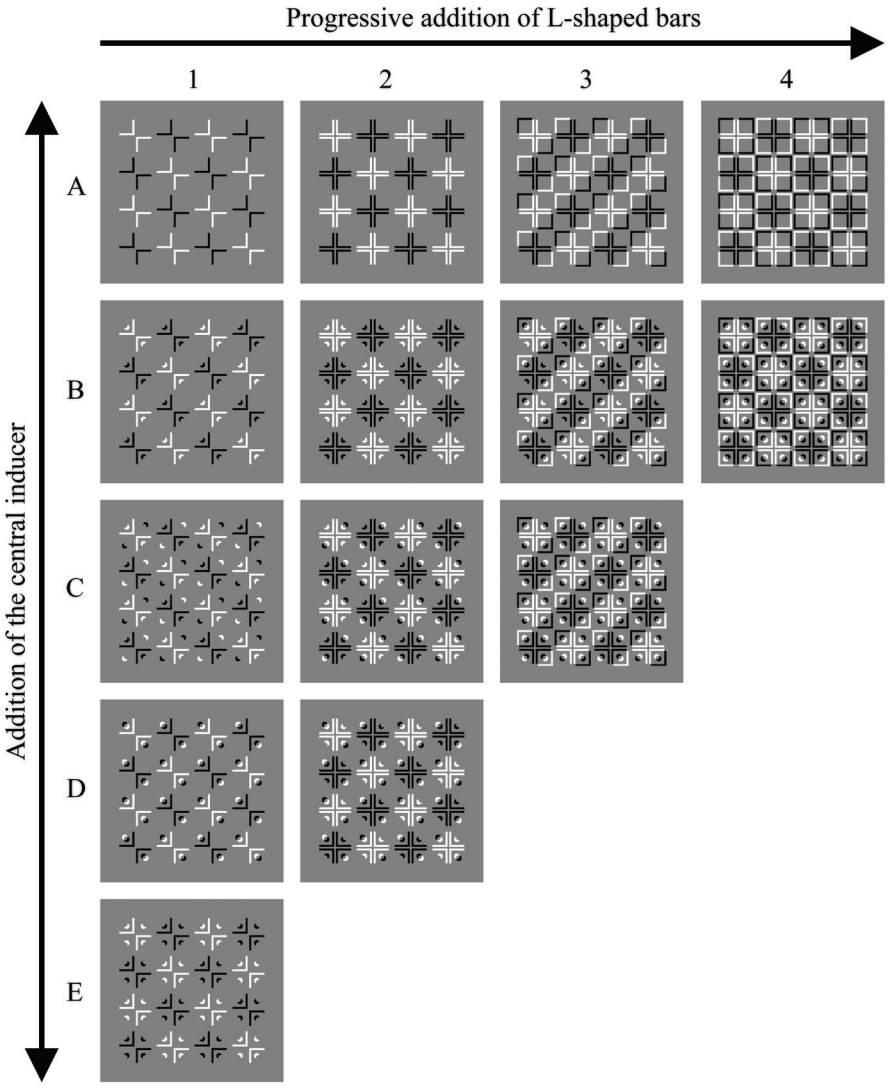

Fig. 28. Decomposition of the contiguous cross shape.

Figure 29 (middle) shows the cross shape in which the basic elements are placed within a certain distance. When the illusion is viewed up close, the completion can still be observed in peripheral vision, indicating long-range interaction between the basic elements. Due to the prolonged separation, lightness assimilation diminishes and may shift toward contrast in the outer gray area where four basic elements meet. The illusory contours flow through the clamps intersecting the two innermost markers and continue outward to the adjacent basic elements via the vertices formed by two L-shaped bars of opposite polarity. The illusory contours are strengthened by the linear organization of basic elements with identical orientation along the diagonal axis.

Figure 29 (right) shows that even when the luminance of the Pisces Starburst – Variant B is homogenized, the central inducer and the orthogonal L-shaped bars still drive the illusory contours in a single direction. Structurally, the open region where the two L-shaped bars meet potentiates a unidirectional contour; likewise, the empty elliptical region between the two circles supports contour formation in only one direction. Scintillations emerge outside the basic elements, concentrated in the midpoint region formed by each group of four basic elements. By changing the background outside the basic elements to neutral gray and adding new markers in the midpoint region, the illusory contours extending outward from the L-shaped bars become sharper and more perceptually salient. When the basic element is completely black, both its internal luminance and the midpoint marker should adjust to white to strengthen the light illusory contours. Conversely, when the basic element is completely white, both its internal luminance and the midpoint marker should adjust to black to strengthen the dark illusory contours.

Citation: Journal of Illusion 2026, **6**: 13831 - https://doi.org/10.47691/joi.v6.13831

The illusion shows certain similarities to Schumann's illusion (Schumann, 1904), Aquarius Starburst – Variant B (Fig. 7, right), which induces illusory contours in a single direction, and Orion Starburst – Variant A, discussed in the next section.

Orion Starburst illusion – Variants A and B

When (1) two layers of the Pisces Starburst – Variant A with opposite polarity (2) are superimposed, and (3) one of the layers is displaced, a novel variant – Orion Starburst – Variant A – emerges with a completely new polarity ordering. The illusion is named the Orion Starburst after the Orion constellation defined by the IAU (Delporte, 1930). For the illusion to work, the line termination of identical polarity must be aligned in a straight line (Fig. 34). The Orion Starburst – Variant B can be created by (1) combining two (2) 45°-rotated basic elements of the Pisces Starburst – Variant B, in which the (3) innermost circles have been replaced with squares. Before they are merged, the direction of the illusory margin – indicated by the yellow dashed lines in Fig. 30 – is adjusted by rotating one of the elements by 90°. The Orion Starburst – Variant B contains not only elements with identical polarity on each side, as in the Pisces Starburst Illusions, but also elements with shifted polarity and higher local contrast, whereas the Orion Starburst – Variant A contains only the shifted-polarity elements with high local contrast.

The Orion Starburst – Variant B consists of two U-shaped forms of opposite polarity; each composed of three sides of identical polarity. Two forms arise depending on the element's polarity ordering, and this order can be inverted to switch between them. The demonstrations in Fig. 31 (left) show that the white and black elements of the Orion Starburst – Variant B can each generate an illusory margin like the Spinnwebfäden illusion (Prandtl, 1927), and that when combined, the effect strengthens through contrast-based lightness–contour coactivation. The illusion exhibits a bidirectional ray-beam effect where the illusory margin extends from corners and line terminations. The effect is strongest when the basic element is (1) rotated by 45° and (2) arranged in an alternating configuration, which means leaving the central space between every four elements empty.

Figure 31 (middle) shows that in a non-alternating arrangement, the black part of the illusion closes into a four-sided square, while the white part preserves its U-shape. As a result, parts with the same contrast polarity are blocked, reducing the grouping of elements with identical polarity and thereby weakening the illusion. Figure 31 (right) shows that when the pattern in the central space is inverted, the part of the illusion sharing the same contrast polarity remains unblocked, allowing the ray-beam effect to persist while also producing an outspread lightness effect, like the Pisces Starburst Illusion. However, this combination does not achieve a favorable spatial frequency of components with identical polarity but instead consists of contrast pairs, which explains the diffuse lightness effect.

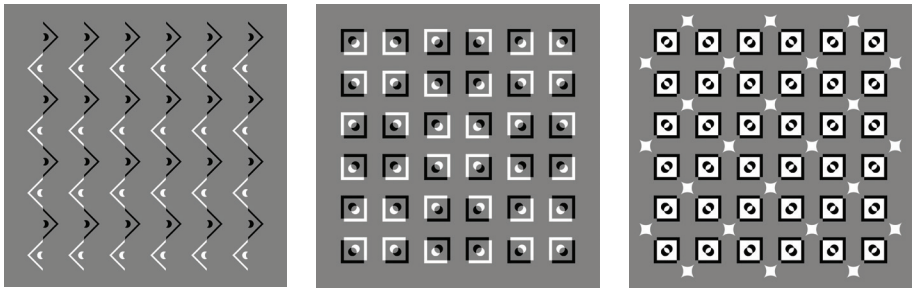

Fig. 29. Left: Zigzag arrangement. Middle: Separation of the basic elements in the contiguous cross shape. Right: Luminance leveling of the basic elements in the Pisces Starburst – Variant B.

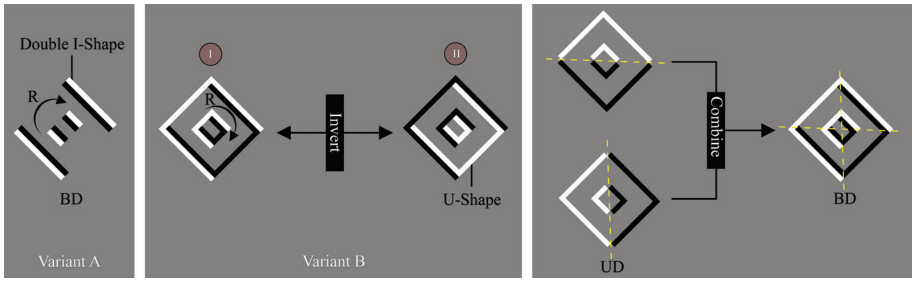

Fig. 30. Basic elements in the Orion Starburst – Variants A and B. R: Rotatable; UD: Unidirectional ray-beam effect; BD: Bidirectional ray-beam effect. The illusory margin along the bisector is indicated by a yellow dashed line.

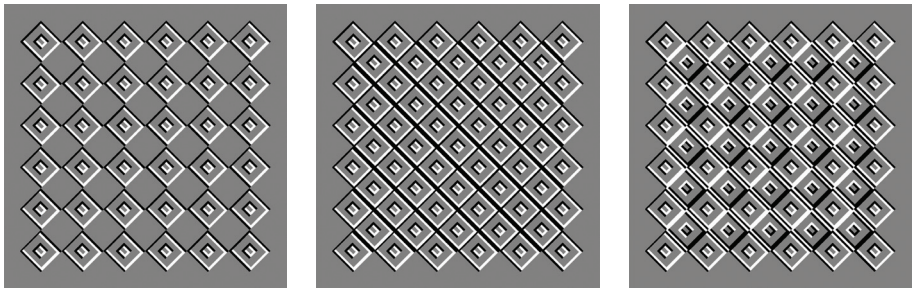

Fig. 31. The left demo shows that both the white and black elements can generate illusory margins on their own, and that the effect intensifies when they are combined. The middle and right demos show blocking and reactivation of the illusion.

When isolating the unblocked fragment of the Orion Starburst – Variant B that contains pairs of lines with homogeneous polarity on each side, the structure transforms into the Pisces Starburst – Variant A. Meanwhile, isolating the fragment with shifted polarity and higher local contrast yields the Orion Starburst – Variant A, which exhibits strong illusory contours extending through the corners and line terminations.

Figure 32 shows that this fragment consists of a pair of Pisces Starburst – Variant A placed side-by-side with a slight interspace. This collided version reveals illusory contours, but it lacks the extended and outspread lightness illusion seen in the Pisces Starburst – Variant A (Fig. 32). Instead, the lightness remains thin and linearly confined along the line terminations in a bidirectional manner, with identical illusory lightness intensity in both directions. Both the Pisces Starburst – Variant A and the collided configuration in Fig. 32 induce geometric distortion, with the vertical axes appearing bent depending on the mirrored arrangement of the basic elements, whereas this effect is absent in Fig. 33. The illusion in Fig. 32 also exhibits a secondary effect that can be described as scintillation flowing through the gray region, arising from (1) the higher local contrast, (2) the thickness of the lines, and (3) the neutral-gray region, similarly to the Enigma illusion (Leviant, 1982).

By placing two basic elements of the Orion Starburst – Variant A in a row without any directional changes, a staircase-like offset between the black and white components is produced, which keeps the edges at the line terminations unchanged. This staircase-like offset creates clear black-and-white corners with opposite orientations in the outer bars, through which the illusory contour passes to the line termination of the inner marker.

Figure 33 (left) shows that when the offset between the two basic elements of the Orion Starburst – Variant A is removed, the illusory contours disappear vertically, horizontally, or both. This indicates that the staircase-like offset between the outermost lines is necessary for corner formation, which, in turn, does not disrupt but induces the illusory contours. Corners with identical polarity and

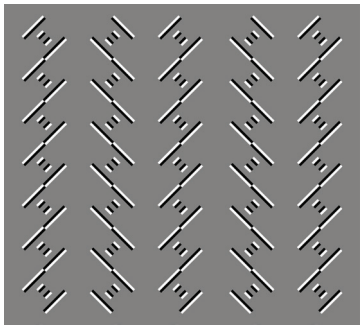

Fig. 32. Two-collided Pisces Starburst – Variant A leads to the Orion Starburst – Variant A.

direction that remain unblocked determine the direction of the ray-beam effect. Figure 33 (middle) shows that when the inner small lines are removed, the illusory contours disappear, while a lightness assimilation becomes notable. Both the outermost bars and the inner markers share the same polarity ordering as the color-reduced Craik–O'Brien–Cornsweet illusion (Cornsweet, 1970) when isolated (Fig. 23), which exhibits lightness assimilation. Figure 33 (right) shows that inverting the polarity of the innermost bars weakens the illusory contours, since the inner and outer bars create opposite illusory lightness. This instead sharpens the edges in areas where: (1) lightness assimilation can still occur or (2) line terminations that remain active. These conditions produce two opposite illusory lightness signals that do not match and therefore reduce the overall intensity. This indicates that a specific polarity ordering is crucial for correcting the lightness of the margins and for evoking a favorable condition that allows corners and line terminations of identical polarity to connect with each other. The illusory margin is darkened when the polarity ordering is white–black–gray–white–black–gray–black–white–gray–black–white, whereas when the sequence is black–white–gray–black–white–gray–white–black–gray–white–black, the illusory margin lightens. Two lightness effects emerge: (1) lightness assimilation appears inside the outer bars and the inner-bar region, which is a duplication of the other. (2)

Citation: Journal of Illusion 2026, **6**: 13831 - https://doi.org/10.47691/joi.v6.13831

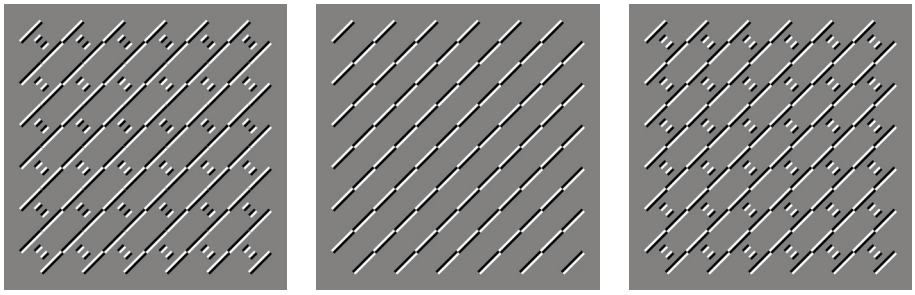

Fig. 33. Orion Starburst – Variant A. Left: Blocking the corners removes the propagation path of the ray-beam effect. Middle: Both parts are required for the illusion to emerge, while the inner markers produce a weak effect. Right: Inverting the inner marker weakens the ray-beam effect.

The illusory contours exhibit a localized lightness effect in a thin band where the contours appear. Surfaces darkened by assimilation show darker illusory contours when the small marker is added, whereas surfaces lightened by assimilation show lighter illusory contours when the small marker is added.

Figures 33 and 34 show that the illusory lightness aligns with the intersecting path between corners and line terminations of identical polarity. Linear organization of black corners and line terminations with identical orientation yields dark contours, whereas linear organization of white corners and line terminations with identical orientation yields light ones. Figure 35 (left) shows that removing the staircase-like offset, due to line extension, weakens contour formation and changes the ray-beam effect in the Pisces Starburst – Variant A to unidirectional.

Figure 35 (middle) presents a new illusion named Pisces Starburst – Variant A (paired outermost-bars version), where each side of the basic element features a pair of outer lines with opposite polarity and an inner line whose polarity matches the nearest outermost bar. The illusion produces a bidirectional ray-beam effect with a diffuse lightness illusion despite the absence of a staircase-based offset. Figure 35 (middle) further indicates that the illusion persists when the innermost markers differ in polarity, while the outermost bars share the same polarity, provided the polarity-reversed innermost markers remain on the same side (black = top left, white = bottom right), facilitating perceptual organization. Figure 35 (middle) shows that the illusion persists and produces a bidirectional ray-beam effect even when the outer bars with identical polarity overlap, are fully parallel, and lack line terminations. The illusion weakens markedly when the outer bars are removed and disappears when the inner markers are removed, while if the innermost bars differ in polarity and the outermost bars share the same polarity, the illusion persists. The ray-beam effect occurs if the inner small bars with differing polarity remain on the same side throughout the entire figure, which facilitates perceptual organization. This

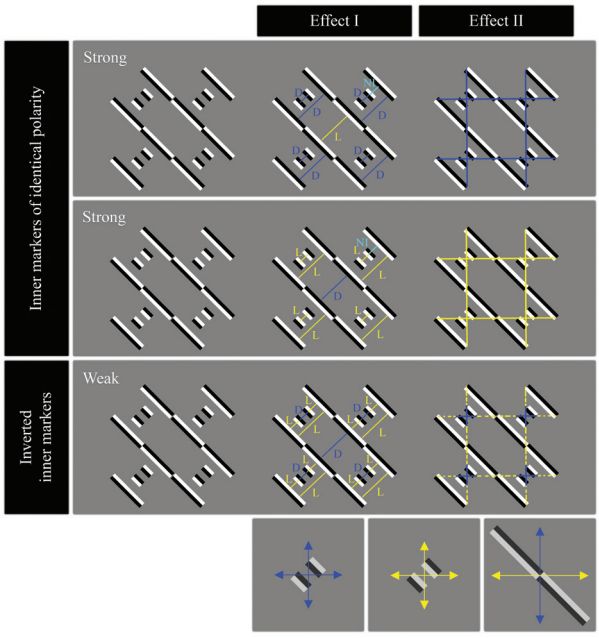

Fig. 34. D = darken, L = lighten, NI = no interaction. Blue arrow = Black corners dominate, producing a dark signal. Yellow arrow = White corners dominate, producing a light signal. Strong effect: When the inner and outer parts generate identical lightness signals. Weak effect: Lightness signals that do not match disrupt the illusion. Effect I: The polarity ordering that evokes assimilation. Effect II: Change in lightness between corners of identical polarity perceived as illusory contours.

indicates that the requirement for inducing the illusion is that the marker must contain elements of opposite polarity while occupying the same location, which allows the pair of opposite-polarity outermost bars to coexist. The change in polarity causes the otherwise weak contours that start from the line's termination of the inner marker to elongate by using the polarity of the outermost bars as support for contour formation. The illusion is strongest when all components are used, while the effect disappears when the inner and outer bars each have uniform polarity but opposite to one another. This unfavorable

polarity arrangement can, in other cases, induce an effect when the smaller marker is placed side-by-side in the middle of the outer bars of opposite polarity. The effect becomes even more visible by creating the outer bars with a staircase-like offset, as shown in the new arrangement named Lattice Illusion in Fig. 35 (right). This illusion evokes change in lightness in the peripheral vision, whereas it disappears under direct fixation, in which the white squares alter a dark illusory contour, and the black corners are perceived as darker. For this illusion to emerge, the (1) inner marker must have opposite polarity, (2) be shorter in length, (3) be positioned side-by-side at the midpoint of the outer lines, and (4) contain corners for effect enhancement. Because the outer bars are longer, only the local region adjacent to the marker of opposite polarity darkens, creating a cross-like effect that also modulates the intensity of the contours generated by the corners.

Figure 36 shows that the bidirectional ray-beam effect in the Pisces Starburst – Variant A and the Orion Starburst – Variants A and B can be transformed into a unidirectional one when the illusions are compressed. The criterion for achieving this is to: (1) ensure that the basic element is shaped as a rhombus or consists of components rotated by 45°. (2) Compressing the width produces a horizontal unidirectional ray-beam, whereas compressing the height produces a vertical one in all three cases.

Those illusions exhibit anisotropic properties, a condition in which the structure displays different characteristics in different directions due to directional deformation, unequal spacing, or non-uniform organization. This anisotropy creates a dominant axis, which, in turn, determines the orientation of the resulting ray-beam effect. The anisotropic effect seen in Fig. 36 can be restored to its normal appearance when subjected to scrolling, subtle shaking, or vibration, a phenomenon that can be described as motion-induced lightness and contour amplification. Rhombus deformation can also be seen in Fig. 5, which does not recover the bidirectional interpretation through shaking alone but instead strengthens the contours that are visible even without shaking.

The mirror inverted T-shape in the Pisces Starburst – Variant B produces a bidirectional ray-beam effect (Fig. 37, left). A 45° rotation, combined with width reduction, yields a horizontally oriented unidirectional ray-beam (Fig. 37, middle), whereas a subsequent 90° rotation restores the illusion to a bidirectional one (Fig. 37, right). This demonstrates that rotation alone, under specific geometric conditions, can add or subtract contours, sharpen the edges, or change lightness effect. A similar condition can also be found in the Hermann–Hering illusion (de Lafuente & Ruiz, 2004), the Pisces Starburst – Variant A, and the Orion Starburst – Variants A and B. The underlying mechanism can be described as angle-induced

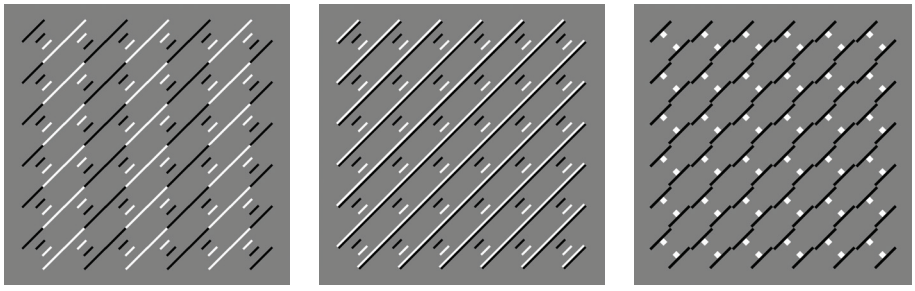

Fig. 35. The left figure shows that the bidirectional contours in the Pisces Starburst – Variant A become unidirectional when two outer lines with the same polarity extend each other; the middle figure shows the paired outer bars version without staircase-like offset; the right figure shows the Lattice illusion producing dark illusory contours.

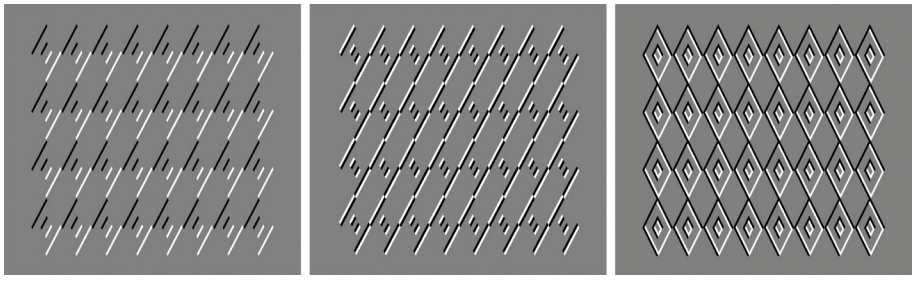

Fig. 36. Anisotropic effect in the Pisces Starburst – Variant A (left), Orion Starburst – Variant A (middle), and Orion Starburst – Variant B (right).

Citation: Journal of Illusion 2026, **6**: 13831 - https://doi.org/10.47691/joi.v6.13831

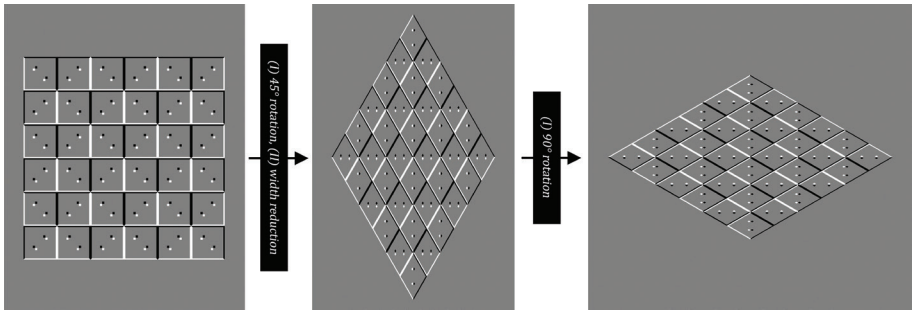

Fig. 37. Angle-induced lightness–contour activation in variant B (innermost clamps version).

lightness–contour activation, in which changes in angle elicit different ray-beam responses.

The strength of Aquarius Starburst A–B, Pisces Starburst A–B, and Orion Starburst A–B changes depending on spatial distance, which causes a mismatch in global and local grouping of elements. For example, in Fig. 14 (middle), lightness assimilation shifts to lightness-contrast when zoomed out (–).

If the innermost markers in the SC of the Pisces Starburst A–B and Orion Starburst A–B are inverted or rotated by 180°, the illusion is canceled; intermediate angles produce the illusion with varying strength, whereas the SC yields the strongest effect.

Discussion

The primary structural labels of the illusions presented in this article – Aquarius, Pisces, and Orion – specify their distinct structural and mechanistic differences and function as subtypes. The secondary family descriptor, Starburst, is inspired by Gianni A. Sarcone's (1993) original Starburst illusion and highlights the similarities among these subtypes, which elicit illusory contours and lightness effects, including the so-called ray-beam effect. The final letter (A–B) serves as a variant code and indicates the differences within each group. When the Hermann grid illusion is rotated by 45°, it transforms into the Spinnwebfäden illusion, attributed to A. Prandtl (1927). Placing small markers of opposite polarity at the center of each diamond in the grid leads to the Aquarius Starburst – Variant A. Transforming the Aquarius Starburst – Variant A into its gradient counterpart yields Vasarely's Nested Squares illusion, thereby demonstrating the structural similarities among these illusions. The Pisces Starburst – Variants A and B are obtained by superimposing two layers of the Aquarius Starburst – Variant A with opposite polarity, while the Orion Starburst – Variants A and B are obtained by superimposing two layers of the Pisces Starburst – Variants A and B with opposite polarity. The superimposition changes both the polarity ordering and the structure of the illusion while still evoking the ray-beam effect. The structural differences between the illusions can be seen through a bar progression with identical polarity in the outer envelope: the Pisces Starburst – Variant A uses a single I-shaped bar, the Orion Starburst – Variant A contains a pair of I-shaped bars, the Pisces Starburst – Variant B a pair forming an L-shape, and the Orion Starburst – Variant B a trio forming a U-shape, whereas the Aquarius Starburst – Variants A and B require a fully closed four-bar configuration. The similarities between the novel Starburst illusions presented in this article are that they use a small inducer pattern placed at the center of the outer envelope, in which the central inducer intensifies or activates the illusion. In addition, the ellipse illusions, which show similarities to the Aquarius Starburst – Variant A, induce changes in lightness within the narrow gap between two ellipses. The placement of a small diamond of opposite polarity adjacent to this gap generates both illusory lightness and contour enhancement. In the Lattice illusion, introduced later in the article, the small white squares attached to the black bars alter a dark illusory contour through the black corners, whereas in the Aquarius Starburst – Variant A, the opposite occurs, in which the black grid and the opposite-polarity central inducer evoke light illusory contours. The Aquarius Starburst – Variant B shows that adding filled, 45° rotated small squares of identical polarity to the grid at its vertices, together with an identical-polarity central inducer, can also reverse the lightness effect, making the white grid lighter and the black grid darker. The Pisces Starburst – Variant A evokes long-range lightness contrast when viewed from afar and assimilation at close distances, while supporting contour formation that extends from the line terminations of identical polarity. The illusory margin in this illusion is supported by contrast-based lightness–contour coactivation, meaning that two illusory contours of opposite polarity can coexist and potentiate each other through the lightness effect. The Orion Starburst – Variant A, which has a similar structure but a new polarity ordering, lacks the outspread lightness illusion seen in Pisces Starburst and instead induces strong illusory contours extending from corners and line terminations of identical polarity, with a lightness effect that

remains thin and linearly confined, similarly to Aquarius Starburst. The Pisces Starburst – Variant B induces strong lightness assimilation, strengthened by a contiguous configuration that supports higher spatial frequencies, polarity-matching enclosure, contrast pair adjacency, and the luminance-contrast convergence effect. This illusion also induces illusory contours that are driven by polarity-unification and that extend from vertices of opposite polarity, corresponding to the region where two L-shaped bars are attached to each other. The Orion Starburst – Variant B not only has difficulty emerging in new configurations but also produces a diffuse illusory lightness. Spinnwebfäden illusion, Aquarius Starburst (A–B), Pisces Starburst (A–B), and Orion Starburst (A–B) are sensitive to deformations that alter the direction of the ray-beams, as well as to angular changes that can subtract or add ray-beams, which can be of interest for further investigation regarding how deformation and angular changes influence the tendency to perceive illusory contours.

References

Adelson, E.H. (2000). Lightness perception and lightness illusions. In M. Gazzaniga (Ed.), *The new cognitive neurosciences* (2nd ed., pp. 339–351). MIT Press.

Brewster, D. (1844). *A notice explaining the cause of an optical phenomenon observed by the Rev. W. Selwyn*. Report of the British Association for the Advancement of Science, Transactions of the Sections, 8, British Association for the Advancement of Science.

Capoot, A. (2023, July 24). Elon Musk rebrands Twitter to 'X', replaces iconic bird logo. *CNBC*. Retrieved from https://www.cnbc.com/2023/07/24/elon-musk-rebrands-twitter-to-x-replaces-iconic-bird-logo.html

Cornsweet, T.N. (1970). *Visual perception*. Academic Press.

de Lafuente, V., & Ruiz, O. (2004). The orientation dependence of the Hermann grid illusion. *Experimental Brain Research, 154*, 255–260. https://doi.org/10.1007/s00221-003-1700-5

Delporte, E. (1930). *Délimitation scientifique des constellations*. Cambridge University Press.

Ehrenstein, W.H. (1941). Über Abwandlungen der L. Hermannschen Helligkeitserscheinung. *Zeitschrift für Psychologie, 150*(1), 83–91. Translated in: Ehrenstein, W.H. (1987). Modifications of the brightness phenomenon of L. Hermann. In S. Petry & G.E. Meyer (Eds.), *The perception of illusory contours* (pp. 35–39). Springer. https://doi.org/10.1007/978-1-4612-4760-9_3

Flaieh, D. [@DFlaieh1987]. (2019, August 14). Invisible line illusion; Aquarius Starburst–Variant A [Post]. *X*. Retrieved from https://x.com/DFlaieh1987/status/1161583914332360704

Flaieh, D. [@DFlaieh1987]. (2024a, August 19). Pisces Starburst–Variant B [Post]. *X*. Retrieved from https://x.com/DFlaieh1987/status/1825603812499009638

Flaieh, D. [@DFlaieh1987]. (2024b, August 19). Pisces Starburst–Variant B [Post]. *X*. Retrieved from https://x.com/DFlaieh1987/status/1825609841269936180

Flaieh, D. [@DFlaieh1987]. (2024c, August 21). Pisces Starburst–Variant A [Post]. *X*. Retrieved from https://x.com/DFlaieh1987/status/1826160065352441927

Flaieh, D. [@DFlaieh1987]. (2024d, September 8). Lightness contrast [Post]. *X*. Retrieved from https://x.com/DFlaieh1987/status/1832880032571600974

Flaieh, D. [@DFlaieh1987]. (2025a, February 20). Pisces Starburst –Variant B: Shape from shading [Post]. *X*. Retrieved from https://x.com/DFlaieh1987/status/1892470241050959919

Flaieh, D. [@DFlaieh1987]. (2025b, August 1). The contrast enhanced ellipse illusion [Post]. *X*. Retrieved from https://x.com/i/status/1951154619863933067

Flaieh, D. [@DFlaieh1987]. (2025c, August 1). The contrast-enhanced ellipse illusion [Post]. *X*. Retrieved from https://x.com/DFlaieh1987/status/1951154769466368184

Flaieh, D. [@DFlaieh1987]. (2025d, November 25). Pisces Starburst–Variant A [Post]. *X*. Retrieved from https://x.com/DFlaieh1987/status/1993255016225030563

Flaieh, D. [@DFlaieh1987]. (2025e, November 25). Pisces Starburst–Variant A [Post]. *X*. Retrieved from https://x.com/DFlaieh1987/status/1993304707012624644/photo/1

Flynn, O., & Shapiro, A.G. (2014). A note concerning the relationship between the Adelson's Argyle illusion and Cornsweet edges.*Psihologija, 47*(3), 353–358. https://doi.org/10.2298/PSI1403353F

Gregory, R.L. (1997). Knowledge in perception and illusion. *Philosophical Transactions of the Royal Society B: Biological Sciences, 352*(1358), 1121–1128. https://doi.org/10.1098/rstb.1997.0095

Hering, E. (1872). Zur Lehre vom Lichtsinne I: Über successive Lichtinduktion. *Sitzungsberichte der Akademie der Wissenschaften Wien, Mathematisch-naturwissenschaftliche Klasse, 66*, 5–24. Reprinted in Zur Lehre vom Lichtsinne: Sechs Mitteilungen (1878). Retrieved from https://www.deutschestextarchiv.de/book/format/html/hering_lichtsinn_1878

Hermann, L. (1870). Eine Erscheinung simultanen Contrastes. *Pflügers Archiv für die gesamte Physiologie, 3*, 13–15. https://doi.org/10.1007/BF01855743

Kanizsa, G. (1976). Subjective contours. *Scientific American, 234*(4), 48–52. https://doi.org/10.1038/scientificamerican0476-48

Kitaoka, A. (2001). Illusion designology (7): Illusory light perception that cannot be explained by Fourier analysis. *Nikkei Science, 31*(8), 66–68.

Koffka, K. (1935). *Principles of gestalt psychology*. Lund Humphries.

Leviant, I. (1982). Illusory motion within still pictures: The L-effect. *Leonardo, 15*(3), 222–223. https://doi.org/10.2307/1574685

Martinez-Conde, S., & Macknik, S.L. (2017). Vasarely's nested squares and the alternating brightness star illusion. In A. Shapiro & D. Todorovic (Eds.), *The Oxford compendium of visual illusions* (pp. 407–414). Oxford University Press. https://doi.org/10.1093/acprof:oso/9780199794607.003.0054

Motokawa, K. (1950). Field of retinal induction and optical illusion. *Journal of Neurophysiology, 13*(6), 413–426. https://doi.org/10.1152/jn.1950.13.6.413

Ninio, J. (2001). Last but not least: Flashing lines. *Perception, 30*, 253–257. https://doi.org/10.1068/p3002no

Pinna, B., & Brelstaff, G.J. (2000). A new visual illusion of relative motion. *Vision Research, 40*(16), 2091–2096. https://doi.org/10.1016/S0042-6989(00)00072-9

Pinna, B., Brelstaff, G., & Spillmann, L. (2001). Surface color from boundaries: A new 'watercolor' illusion. *Vision Research, 41*(20), 2669–2676. https://doi.org/10.1016/S0042-6989(01)00105-5

Prandtl, A. (1927). Über gleichsinnige Induktion und die Lichtverteilung in gitterartigen Mustern. *Zeitschrift für Sinnesphysiologie, 58*, 263–307.

Citation: Journal of Illusion 2026, **6**: 13831 - https://doi.org/10.47691/joi.v6.13831

Ramachandran, V.S. (1988). Perception of shape from shading. *Nature, 331*(6152), 163–166. https://doi.org/10.1038/331163a0

Redies, C., & Spillmann, L. (1981). The neon color effect in the Ehrenstein illusion. *Perception, 10*, 667–681. https://doi.org/10.1068/p100667

Roncato, S. (2017). Geometrical errors are the cost of maintaining the luminance contrast polarity. In A.G. Shapiro & D. Todorović (Eds.), *The Oxford compendium of visual illusions* (Chap. 32). (pp. 290–294). Oxford University Press. https://doi.org/10.1093/acprof:oso/9780199794607.003.0032

Roncato, S., Guidi, S., Parlangeli, O., & Battaglini, L. (2016). Illusory streaks from corners and their perceptual integration. *Frontiers in Psychology, 7*, 959. https://doi.org/10.3389/fpsyg.2016.00959

Sarcone, G.A. (1993). *Scintillating Starburst illusion*. Archimedes Lab. [Workshop notes / early publication].

Sarcone, G.A. (2021, June 30). *Scintillating Starburst illusion*. Gianni Sarcone – Archimedes Lab. Retrieved from https://www.giannisarcone.com/Scintillating_starburst.html

Schachar, R.A. (1976). The 'pincushion grid' illusion. *Science, 192*(4237), 389–390. https://doi.org/10.1126/science.1257775

Schumann, F. (1904). Beiträge zur Analyse der Gesichtswahrnehmungen. IV. *Zeitschrift für Psychologie, 36*, 161–185.

Somers, D.C., & Adelson, E.H. (1997). Junctions, transparency and brightness. *Investigative Ophthalmology & Visual Science (Supplement), 38*, S453.

Tyler, C.W. (2000). The Gingham illusion: Scintillations and the depth representation of second-order signals. *Investigative Ophthalmology & Visual Science, 41*(4), S228.

van Tuijl, H.F.J.M. (1975). A new visual illusion: Neon-like color spreading and complementary color induction between subjective contours. *Acta Psychologica, 39*(6), 441–445. https://doi.org/10.1016/0001-6918(75)90042-6

Varin, D. (1971). Fenomeni di contrasto e diffusione cromatica nell'organizzazione spaziale del campo percettivo. *Rivista di Psicologia, 65*, 101–128.

Vasarely, V., & Joray, M. (1970). *Vasarely II*. Editions du Griffon.

Vicario, G.B. (2009). *Illusioni ottiche geometriche*. Istituto Veneto di Scienze, Lettere e Arti.

Zavagno, D. (1999). Some new luminance-gradient effects. *Perception, 28*(8), 835–838. https://doi.org/10.1068/p2633